

# Contact numbers in packings of frictional cylinders

Matthias Schröter<sup>1,\*</sup>, Cyprian Lewandowski<sup>1,2,3</sup>, and Max Neudecker<sup>1</sup>

<sup>1</sup>Max Planck Institute for Dynamics and Self-Organization, 37077 Göttingen, Germany

<sup>2</sup>National High Magnetic Field Laboratory, Tallahassee, Florida, 32310, USA

<sup>3</sup>Department of Physics, Florida State University, Tallahassee, Florida 32306, USA

**Abstract.** The mechanical stability of a granular system depends on the average number of contacts  $Z$  between its particles. For most particle shapes, predicting  $Z$  as a function of the average volume fraction  $\phi$  is complicated by the spatial correlations between simultaneously contacting particles. However, in the dilute packings formed by cylinders with large aspect ratios  $\alpha$  (length of the cylinder divided by its diameter) the individual contacts can be expected to become uncorrelated. Philipse (Langmuir **12**, 1127 (1996)) derived from this idea the Random Contact Model (RCM) which predicts  $Z_{RCM} = 2\alpha\phi$ . Here we compare  $Z_{RCM}$  with X-ray tomography measurements of  $Z(\alpha, \phi)$  in cylinder packings with  $\alpha =$  of 14.1, 21.1, and 28.2. We find the measured  $Z$  to be smaller than  $0.85 Z_{RCM}$ . Using a Voronoi tessellation we then analyze  $Z$  as a function of  $\phi$  on the level of individual particles where the linear relationship does not hold up.

## 1 Introduction

Granular materials are ubiquitous in our daily lives. However, their athermal and dissipative nature has up to now impeded the evolution of a comprehensive theory. Even the more limited question of the conditions and limits of mechanical stability of packings is still far from settled. We know that the average number of contacts  $Z$  has to be above the so called isostatic threshold  $Z_{iso}$  in order to fix all the rotational and translational degrees of freedom of the particles, which is the commonly used definition of mechanical stability. At the same time there is a maximal average number of contacts  $Z_{max}$  which derives from the fact that contacts also are geometric constraints on the particle coordinates and that this system can not be overdetermined. What complicates the situation is that the values of  $Z_{max}$  and  $Z_{iso}$  depend on the particle shape and that  $Z_{iso}$  depends additionally on the presence or absence of interparticle friction  $\mu$ , as shown in table 1.

**Table 1.** The range of contact numbers of mechanically stable packings depends on the particle shape and the interparticle friction  $\mu$  [1, 2] See also review [3] and references therein.

	$Z_{iso}^{\mu=0}$	$Z_{iso}^{\mu=\infty}$	$Z_{max}$
spheres	6	4	6
cylinders	10	4	10

While the second column of table 1 displays  $Z_{iso}$  values for particles with infinite  $\mu$ , the  $Z_{iso}$  values for real world particles, which typically have  $\mu$  values between 0.2 and 0.8, do not differ too much. For example, spheres with  $\mu = 0.75$  have a  $Z_{iso}$  of smaller than 4.5 [4]. A consequence

of the different values of  $Z_{iso}^{\mu=\infty}$  and  $Z_{max}$  is that experimental packing, which by definition involve frictional particles, will always exist over a range of volume fractions  $\phi$  (defined as particle volume divided by total volume). Increasing  $\phi$  will move particles on average closer together and therefore also increase  $Z$ . While there are some numerical insights [5], there is no first principle based theory describing how  $Z$  depends on  $\phi$  for a given shape, value of  $\mu$ , and protocol used for the compaction [6].

In contrast, many numerical and theoretical studies assume particles to be frictionless. Assuming that the particles are also incompressible, this fixes the  $Z$  value of the packings to  $Z_{iso}^{\mu=0} = Z_{max}$ .

In the absence of a general theory, it can be helpful to study the limiting cases of a problem. One of them are packings of cylinders with large aspect ratios  $\alpha$  (defined as the length of the cylinders divided by their diameter). A cylinder with  $\alpha = 10$  has about 74 % more surface area than a sphere of the same volume. This larger surface area translates into more possibilities to form a contact, consequently mechanical stability occurs already at lower values of  $\phi$ . And this effect becomes stronger with increasing  $\alpha$ . Therefore, the larger  $\alpha$  gets, the larger is the spatial separation between the individual contacts. This reduces the geometric constraints the contacting particles impose on each other. This approximation of ignoring those constraints completely forms the basis of the Random Contact Model (RCM) for cylinders.

### 1.1 The Random Contact Model

This model suggested by Philipse [7, 8] is based on a mean field argument and does not enforce mechanical stability: Imagine a fixed test cylinder and a neighboring cylinder

\*e-mail: matthias.schroeter@ds.mpg.de

at distance  $\vec{r}$ . The probability  $f_{ex}(\vec{r})$  that neighbor and test cylinder overlap, is then interpreted as the probability that they form a contact. Using the mean field approximation that the number density  $\rho$  does not depend on  $\vec{r}$  (i.e. that the different contacting particles do not influence each other), which becomes reasonable for large  $\alpha$ , we obtain:

$$Z = \int f_{ex}(\vec{r}) \rho(\vec{r}) d\vec{r} \approx \rho \int f_{ex}(\vec{r}) d\vec{r} \quad (1)$$

The second integral is the orientational averaged excluded volume  $V_{ex}$ . With the definition  $\phi = \rho V_{cyl}$  we obtain:

$$Z = \phi \frac{V_{ex}}{V_{cyl}} \quad (2)$$

Using Onsager's result[9] for  $\frac{V_{ex}}{V_{cyl}}$ :

$$\frac{V_{ex}}{V_{cyl}} = \frac{6\alpha^2 + 24\alpha + 16}{2 + 3\alpha} \quad (3)$$

we finally derive in the limit of large  $\alpha$ :

$$Z_{RCM} = 2\alpha\phi \quad (4)$$

describing how the contact number in cylinder packings should depend on both the aspect ratio and the density.

## 1.2 Previous studies of cylinder packings

Cylinders are a frequently used model system for a non-spherical granular medium, for a recent review see [10]. Previous numerical tests of eq. 4 used frictionless cylinders in which case  $Z_{iso}^{\mu=0} = Z_{max} = 10$  and eq. 4 turns into  $\phi = 5/\alpha$ . This scaling has indeed been approximately confirmed [11–13].

Experiments measuring only  $\phi$  and  $\alpha$  [7, 8, 14] also confirmed  $\phi \sim 1/\alpha$  with a prefactor compatible with  $Z = 10$ , albeit with large uncertainties. The only previous study that measured  $\phi$ ,  $Z$ , and  $\alpha$  simultaneously [1] prepared packings with  $\alpha = 15, 32$  to  $50$  at different  $\phi$  values each. They found  $Z$  values in the range of  $6.5$  to  $9.8$ , and in general to be  $50$  to  $90\%$  of the value expected according to eq. 4.

## 2 Experimental setup

Cylindrical particles are cut from longer strands of a composite material consisting of several micron large carbohydrate granules embedded in an amorphous protein matrix [15] (Spaghettini Barilla n. 3). Three different lengths are prepared:  $2$  cm (4800 particles),  $3$  cm (2000 particles), and  $4$  cm (1040 particles) The dimensions of 50 samples of nominally  $4$  cm length are measured using a micrometer screw gauge resulting in a length of  $40 \pm 0.3$  mm, and a diameter of  $1.42 \pm 0.02$  mm. In consequence, the cylinders have aspect ratios  $\alpha$  of  $14.1, 21.1$  and  $28.2$ .

Packings are prepared in a plexiglass cylinder of diameter  $12$  cm and height  $30$  cm; this cylinder is filled from a tube (inner diameter =  $10.3$  cm) with pegs attached to the exit. To reduce the alignment of the particles with

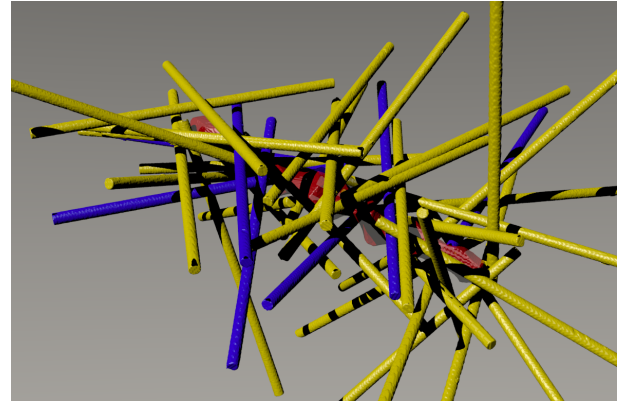


**Figure 1.** Rendering of a tomography result using cylinders with an aspect ratio of 28. The Voronoi cell of the central cylinder is shown in red. Blue cylinders are contact with central cylinder, yellow ones contribute to the faces of the Voronoi cell.

the boundaries, the base of the container is made from randomly aligned cylinders embedded in a floral foam. Though all particles are detected and used for the analysis, the results discussed below consider only cylinders which come nowhere closer to the boundary than one particle length.

For each aspect ratio two distinct samples are prepared and then X-ray tomographies are taken with a Nanotom (GE sensing and inspection). The spatial resolution of the tomograms is  $96.8 \mu\text{m}$  ( $4$  cm) and  $100 \mu\text{m}$  per voxel ( $2$ cm and  $3$  cm) which results in three-dimensional images with on average  $1150 \times 1150 \times 700$  voxel<sup>1</sup>. After the initial tomography the sample container is mounted on an electromagnetic shaker and a series of sinusoidal taps with a maximal acceleration of  $2g$  and a repetition frequency of  $3$  Hz is applied. After each  $10, 100, 1000$ , and  $10000$  taps another tomogram is taken.

### 2.1 Identifying particles

The three-dimensional tomographies are segmented in a three step process. First, each tomogram is binarized twice: a) using a local threshold computed with the Bradley method applied to a  $20 \times 20$  two-dimensional neighborhood [16] and b) using a global threshold based on Otsu's [17]) method. Only voxel which are above both thresholds are considered as belonging to the cylinders.

The second step is an Euclidean distance transform of the the binarized tomogram; the result is then used for an erosion (removal of voxels close to a surface) which separates touching cylinders. Using the default labeling method of Matlab, individual cylinders are identified as groups of connected voxels. This approach achieves a detection rate of  $99.88\%$ .

In the third step their center of mass and the orientation of each voxel croup is used to create a virtual cylinder with a individually controlled radius and length. These two parameters are then iteratively optimized to maximize

<sup>1</sup>An animated zoom through a packing can be found at <https://www.youtube.com/watch?v=76Z1Bbj7CtQ>

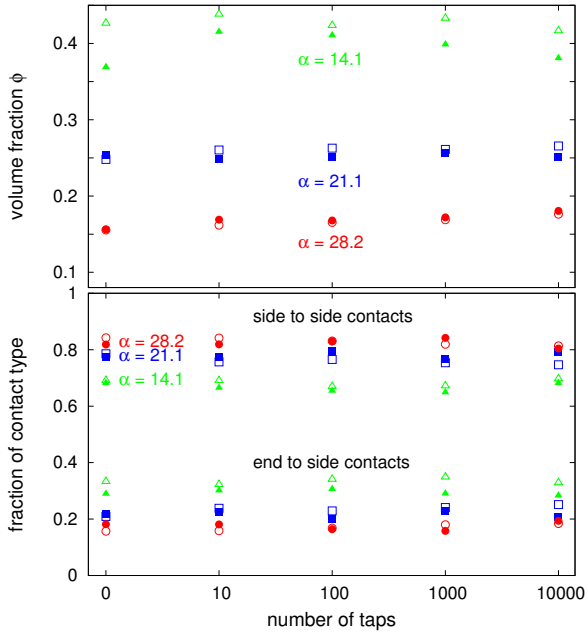


**Figure 2.** Preparation of experimental cylinder packings by tapping. (top) At the applied tapping strength of 2 g only the longest particles do compactify consistently with the number of applied taps. Open and closed symbol correspond to two individual runs. (bottom) Contribution of the two dominant contact types. The third possible type, end to end contacts, accounts for less than 0.74 % of the total contacts and is not shown here.

the percentage of virtual voxels overlapping with true voxels in the binarized image before erosion. In the case of  $\alpha = 28.2$ , the so created virtual cylinders have diameters of  $1.419 \pm 0.019$  mm and lengths of  $39.9 \pm 0.3$  mm, which is in good agreement with our separate measurements of their geometry.

## 2.2 Determining contacts and Voronoi volumes

The identification of particle contacts in experimental images of packings is always complicated by the finite resolution of those images. In order to obtain optimal results, we use the method described in [18] where particle radii are grown by a small factor which is determined by modelling the statistical likelihood of the observed contact number. Since the number of end to end contacts is negligible, only the radius is adjusted.

Voronoi cells are determined with a self-written tessellation algorithm where each voxel is assigned to the the cylinder with the closest surface voxel. Figure 1 displays a detail from an analyzed packing.

## 3 Experimental results

Tapping a granular sample in order to increase  $\phi$  is a frequently applied method and has also been used successfully for cylinders [1, 19]. However, as shown in figure 2 a), we succeed only for  $\alpha = 28.2$  in compactifying the sample systematically. The other four samples display random fluctuations in  $\phi$ , which evidences reorientation of the

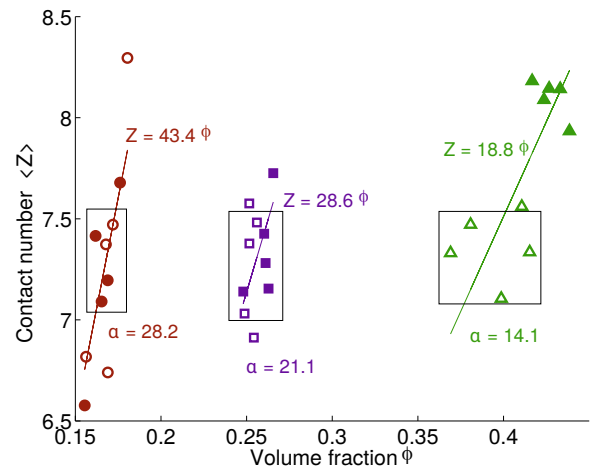


**Figure 3.** Contact number in frictional cylinder packings increase with  $\phi$ . Open and closed symbols correspond to the two experiments displayed in figure 2. Straight lines are linear fits meant for comparison with the RCM. Data points inside the black boxes correspond to the tomograms used for the local analysis shown in figure 4.

particles, but no monotonic compaction. Given the different focus of our study, we did not explore which range of tapping parameters would compactify these samples.

The derivation of eq. 4 was not concerned with mechanical stability, so we still need to require that  $Z$  is larger than  $Z_{iso}$ , which for frictional cylinders is 4. Figure 3 shows that this is indeed the case. Our range of  $Z$  values is about 45 % smaller than the one measured in [1], which corresponds to the fact that their compaction protocol was more efficient than ours.

Figure 2 bottom shows that the majority of the contacts are side to side contacts with a proportion increasing with  $\alpha$ . The absolute numbers are in a good agreement with an extrapolation of the simulation results reported in [20].

While figure 3 is quite noisy, testing equation 4 by fitting the data with  $Z = k\phi$  is not unreasonable. However, the  $k$  values shown in figure 3 amount to only 67% ( $\alpha = 14.1$ ) to 77% ( $\alpha = 28.2$ ) of the values expected according to the RCM model. Similar discrepancies have also been reported in [1].

The most generic hypothesis explaining this discrepancy is that the assumptions of the RCM (constant number density  $\rho$ , approximation of equation 3) are not yet fulfilled for the  $\alpha$  values studied here. Reference [1] reports indeed a 98 % agreement with the RCM prediction for cylinders with  $\alpha = 50$ . A second possible explanation is the fact that in the RCM contacts are defined as overlap between cylinders, not touching. This introduces a steric hindrance between particles which in turn modifies the contact number distribution [21].

### 3.1 A local test of the RCM

Equation 4 is based on a mean-field argument, it should therefore also work on a local level. To test this, we com-

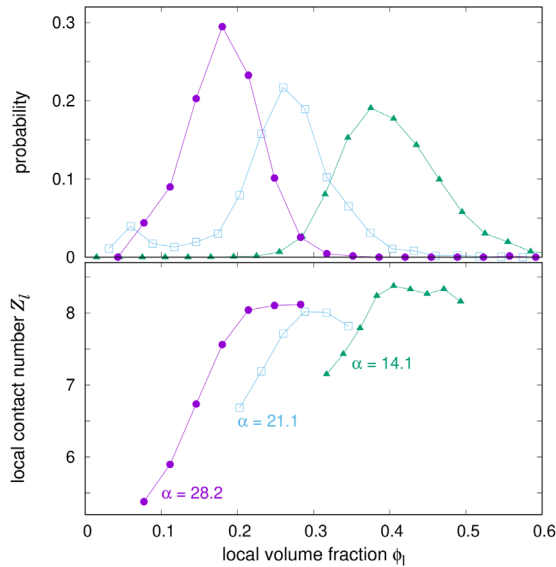


**Figure 4.** For each aspect ratio, there is a saturation in the number of contacts a cylinder makes as a function of the local volume fraction  $\phi_l$  of the cylinders. (top) shows the distribution of  $\phi_l$ , computed using the Voronoi volumes of the cylinders. (bottom) displays the average contact number of all cylinders belonging to a given bin in  $\phi_l$ .

pute for each of the cylinders a local volume fraction  $\phi_l$  as the ratio of the cylinder volume divided by its Voronoi volume. By binning the cylinders in  $\phi_l$  and computing the average contact number  $Z_l$  of these bins, we can test if  $Z_l$  is proportional to  $\phi_l$  as implied by the RCM. As shown in figure 4 this is not the case, there are clear plateaus in  $Z_l$  for the particles with the largest  $\phi_l$ .

These plateaus are responsible for measured  $Z$  values being smaller than the one predicted by the RCM. The change of the plateau length with  $\alpha$  is also compatible with the assumptions that cylinders with even larger  $\alpha$  values will be described better by the RCM. Both the width and height of these plateaus is not explained by present theories; so more work is required.

We thank Sebastian Pitikaris for experimental support and Claus Heussinger and Pascal Wieland for illuminating discussions. C.L. acknowledges support from the 2013 DAAD RISE fellowship

## References

[1] J. Blouwolf, S. Fraden, The coordination number of granular cylinders, *Europhysics Letters* **76**, 1095 (2006). [10.1209/epl/i2006-10376-1](https://doi.org/10.1209/epl/i2006-10376-1)

[2] R.C. Ball, R. Blumenfeld, Stress Field in Granular Systems: Loop Forces and Potential Formulation, *Physical Review Letters* **88**, 115505 (2002).

[3] M. van Hecke, Jamming of soft particles: geometry, mechanics, scaling and isostaticity, *J. Phys.: Condens. Matter* **22**, 033101 (2010).

[4] F.M. Schaller, M. Neudecker, M. Saadatfar, G.W. Delaney, G.E. Schröder-Turk, M. Schröter, Local

Origin of Global Contact Numbers in Frictional Ellipsoid Packings, *Physical Review Letters* **114**, 158001 (2015). [10.1103/PhysRevLett.114.158001](https://doi.org/10.1103/PhysRevLett.114.158001)

[5] A. Baule, R. Mari, L. Bo, L. Portal, H.A. Makse, Mean-field theory of random close packings of axisymmetric particles, *Nature Comm.* **4**, 2194 (2013). [10.1038/ncomms3194](https://doi.org/10.1038/ncomms3194)

[6] M. Schröter, A local view on the role of friction and shape, *EPJ Web of Conferences* **140**, 01008 (2017). [10.1051/epjconf/201714001008](https://doi.org/10.1051/epjconf/201714001008)

[7] A.P. Philipse, The random contact equation and its implications for (colloidal) rods in packings, suspensions, and anisotropic powders, *Langmuir* **12**, 1127 (1996). [10.1021/la950671o](https://doi.org/10.1021/la950671o)

[8] A.P. Philipse, *Langmuir* **12**, 5971 (1996).

[9] L. Onsager, The Effects of Shape on the Interaction of Colloidal Particles, *Annals of the New York Academy of Sciences* **51**, 627 (1949).

[10] T. Börzsönyi, R. Stannarius, Granular materials composed of shape-anisotropic grains, *Soft Matter* **9**, 7401 (2013). [10.1039/C3SM50298H](https://doi.org/10.1039/C3SM50298H)

[11] S.R. Williams, A.P. Philipse, Random packings of spheres and spherocylinders simulated by mechanical contraction, *Phys. Rev. E* **67**, 051301 (2003).

[12] A. Wouterse, S. Luding, A.P. Philipse, On contact numbers in random rod packings, *Granular Matter* **11**, 169 (2009). [10.1007/s10035-009-0126-6](https://doi.org/10.1007/s10035-009-0126-6)

[13] D. Rodney, M. Fivel, R. Dendievel, Discrete Modeling of the Mechanics of Entangled Materials, *Physical Review Letters* **95**, 108004 (2005).

[14] K. Desmond, S.V. Franklin, Jamming of three-dimensional prolate granular materials, *Phys. Rev. E* **73**, 031306 (2006). [10.1103/PhysRevE.73.031306](https://doi.org/10.1103/PhysRevE.73.031306)

[15] J.E. Dexter, B.L. Dronzek, R.R. Matsuo, Scanning electron microscopy of cooked spaghetti, *Cereal Chem.* **55**, 23 (1978).

[16] D. Bradley, G. Roth, Adaptive thresholding using integral image, *Journal of Graphics Tools* **12**, 13 (2007). [10.1080/2151237X.2007.10129236](https://doi.org/10.1080/2151237X.2007.10129236)

[17] N. Otsu, A threshold selection method from gray-level histograms, *IEEE Transactions on Systems, Man, and Cybernetics* **9**, 62 (1979).

[18] F.M. Schaller, M. Neudecker, M. Saadatfar, G. Delaney, K. Mecke, G.E. Schröder-Turk, M. Schröter, Tomographic analysis of jammed ellipsoid packings, *AIP Conference Proceedings* **1542**, 377 (2013). [10.1063/1.4811946](https://doi.org/10.1063/1.4811946)

[19] Y. Fu, Y. Xi, Y. Cao, Y. Wang, X-ray microtomography study of the compaction process of rods under tapping, *Physical Review E* **85**, 051311 (2012). [10.1103/PhysRevE.85.051311](https://doi.org/10.1103/PhysRevE.85.051311)

[20] J. Zhao, S. Li, R. Zou, A. Yu, Dense random packings of spherocylinders, *Soft Matter* **8**, 1003 (2012). [10.1039/C1SM06487H](https://doi.org/10.1039/C1SM06487H)

[21] A. Ekman, A. Miettinen, T. Tallinen, J. Timonen, Contact Formation in Random Networks of Elongated Objects, *Physical Review Letters* **113**, 268001 (2014). [10.1103/PhysRevLett.113.268001](https://doi.org/10.1103/PhysRevLett.113.268001)